Ciliated Sensory Neuron Defects in Caenorhabditis elegans

Author: Colin John Huguenel

Boston College
The College of Arts and Sciences
Biology Department

Ciliated Sensory Neuron Defects in *Caenorhabditis elegans*

Colin J. Huguenel

April 2008

Ciliated Sensory Neuron Defects in *Caenorhabditis Elegans*

Colin J. Huguenel

Advisor: Dr. John Wing, Ph.D.

Abstract

Presented here is research investigating genes that are involved in the development and maintenance of ciliated nerve endings in the nematode *Caenorhabditis elegans.*
C. elegans utilizes a subset of neurons, referred to as ciliated sensory neurons, to sense certain changes in its environment. There are two amphid sensilla (sense organs) that mediate exposure of these ciliated endings to the animal's external environment. Those ciliated endings that penetrate the cuticle are responsible for a myriad of behaviors that range from chemotaxis to osmotic avoidance, but in general function for the reception of environmental cues and stimuli. The intraflagellar transport (IFT) process facilitates the morphogenesis of these ciliated endings, and animals lacking intact ciliated endings may not be able to detect nourishment, hazardous environments, or other worms for mating.

Mutant strains used in this study were generated by EMS mutagenesis of wild-type N2 animals and a subsequent screen of those worms displaying significant cilia dysfunction as evidenced by their dye-filling defective (Dyf) phenotype. Cilia-mediated uptake of lipophilic DiI into six pairs of amphid sensory neurons and two pairs of phasmid sensory neurons is expected in wild-type (N2) animals, but in Dyf animals, this dye-filling is disrupted, either through morphological defects, or deleterious mutations in the IFT process.

To investigate the morphogenesis of cilia in *C. elegans*, we analyzed two specific mutant strains, WX737 *dyf-3(og022)*IV and PK841 *dyf-15(pk841)*V, that are defective in the uptake of fluorescent dye DiI and abnormal in sensory cilium structure. Through a variety of genetic mapping techniques, we were able to successfully map experimental gene *dyf-15(pk841)* to an interval of 2.84cM on chromosome V, and identify *og022* as an allele of the gene *dyf-3*. It has been previously shown that *dyf-3* expression is detected in 26 chemosensory neurons, including six IL2 neurons, eight pairs of amphid neurons (ASE, ADF, ASG, ASH, ASI, ASJ, ASK and ADL) and two pairs of phasmid neurons (PHA and PHB). Analysis of cilium malformation and the presence of a recognition sequence for the DAF-19 transcription factor suggest that *dyf-3* is involved in the intraflagellar transport system complex B.

Acknowledgments

I would like to sincerely thank everyone who contributed to this work, without all of you this endeavor would not have been a success.

I would first like to thank Dr. John Wing for his continued guidance in researching and writing this thesis, for the many valuable discussions that have taught me about what it means to be a scientist, and for his help in keeping our lab functioning and productive throughout a difficult time.

While working on this project, I have been fortunate to work with a number of fantastic scientists and researchers from whom I have learned a great deal. I would like to thank Dr. Michael Reardon for his continued support and guidance in developing the direction for this project, and Dr. Howard Chen for his invaluable advice. In addition I would like to thank all of my undergraduate colleagues: Sarah Fenerty, Christina Kearney, Nick Lekic, Allison Sheffield, and Patrick McKenzie, for their assistance and conversation, but mostly their sanity in an insane situation.

Above all else, I would like to thank my family for their undying support during this project, and during all the steps in my life that have led me here. I owe everything that I am to their advice, love, and devotion. Without the opportunities you all have provided for me, I would not have been able to pursue my passions to the extent that I have. Mom, thank you for keeping me grounded and giving me perspective in some of the most stressful moments of my life. Dad, thank you for inspiring me to pursue the field that I am in today, and for giving me the undying passion for investigation, research, and an insatiable curiosity about life. I love you all dearly, and words cannot express my gratitude.

Table of Contents

I. Introduction

Background

The soil nematode *Caenorhabditis elegans* is a small (1.5mm long adult), unsegmented, worm-like, bilaterally symmetrical animal that possesses many of the same organ systems as other animals, including nervous, digestive, and reproductive systems. The species exists as a hermaphroditic sex with a very small male population that makes up about 0.1% of the total on average. Males are equipped with a single-lobed gonad and vas deferens, as well as a specialized and distinctly noticeable tail for mating. Members of the hermaphrodite population, however, have two ovaries, oviducts, spermatheca, and a single uterus. Eggs are laid strictly by the hermaphrodite and, after hatching, progress through four distinct larval stages (L1 through L4) before reaching adulthood. In the L4 stage, the hermaphrodite will begin producing all of its sperm, and then begins producing oocytes once it reaches adulthood. After self-insemination, wild-type hermaphrodites can lay close to 300 eggs, while hermaphrodites fertilized by male individuals can lay a far greater number. Kept at room temperature, strains can have a life-span of 3-4 weeks and a life cycle of approximately 4 days.[1]

C. elegans is useful as a laboratory model system for a variety of reasons. Strains are cheap and easy to maintain, feeding off *Escherichia coli* bacterial lawns grown up on NGM media, and can be frozen indefinitely at -80°C, allowing for the ease of long-term storage and archival.[1] Most of the early knowledge assembled about *C. elegans* was facilitated by the determination of the complete wild-type cell lineage by observation of cell divisions and migrations.[2] As opposed to more complex organisms, these discreet cell lineages in the nematode have a largely invariant developmental fate, allowing for

the animal's cellular differentiation from fertilization to adulthood to be studied in great detail. In addition to these benefits, *C. elegans* was the first multicellular organism to have its genome completely sequenced. Published in 1998, the 100 million base-pair genome containing an estimated 20,000 genes is spread across five pairs of autosomes and one X sex chromosome.[3] This deep understanding of the cellular and genomic structure of the animal combined with it's short life cycle offers a great potential for complex genetic analysis through various techniques.

C. elegans Neurobiology

In our laboratory, *C. elegans* is useful because it is one of the simplest organisms to possess a fully operational nervous system. In hermaphrodites, the complete connectivity of the 302 existing neurons has been mapped out, allowing comprehensive genetic research to be conducted into their structure and function. *C. elegans* utilizes a specialized subset of neurons, referred to as ciliated sensory neurons, to sense certain changes in its environment. There are two bilaterally symmetrical amphid sensilla (sense organs) and each contains the endings of 12 types of sensory neurons. The 12 neurons in each amphid are distinct both in morphology and in interneuron connectivity; however, each is bipolar with a sensory process (dendrite) and a presynaptic process (axon) that extend from the cell body. Dendrites extend all the way to the tip of the head of the animal where they end in sensory cilia roughly 5μm long, whereas axons extend to the nerve ring to enhance connectivity with the rest of the nervous system. The amphids mediate exposure of the neurons' ciliated endings to the animal's external environment, and those ciliated endings that penetrate the cuticle are responsible for a myriad of

behaviors that range from chemotaxis to osmotic avoidance. Eight of the sensory neurons (ADF, ADL, ASE, ASG, ASH, ASI, ASJ, ASK) have just such cilia that extend through the amphid pore and are exposed to the outside environment where they mostly detect water-soluble substances.[4] Animals lacking intact ciliated endings may not be able to detect nourishment, hazardous environments, or other worms for mating.

IFT Process maintains cilia morphogenesis

Microtubule based cilia are microscopic cellular extensions that aid in a variety of cellular roles including motility, developmental aspects, and sensory functions.[5,6] Sensory cilia in multicellular organisms, such as *C. elegans*, are non-motile in function and often constructed as extensions at the apical end of sensory neurons. These aforementioned ciliated sensory neurons are specialized for a variety of sensory capacities, and in the case of *C. elegans*, require correct localization of olfactory receptors in order to process chemical cues from the environment, such as food, mates, water soluble and volatile compounds.[7,8]

A microtubule-based intraflagellar transport (IFT) system conveys the proteins required for the generation and maintenance of these ciliated sensory neurons in the form of cargo complexes A and B. Two different microtubule-based motors facilitate movement of these IFT cargo complexes along the microtubule; the anterograde motor is kinesin-II, and the retrograde motor is dynein 1b.[9-13] IFT particles carry axonemal subunits to the site of assembly at the tip of the axoneme; thus, IFT is necessary for axonemal growth.[11,13] Therefore, since the axoneme needs a continually fresh supply of proteins, an axoneme, such as a ciliated sensory neuron, with defective IFT machinery

will slowly shrink in the absence of replacement protein subunits. Much of our understanding of the IFT process and the mechanisms that govern it was a result of in depth study of motile flagella morphogenesis in *Chlamydomonas reinhardtii*.[14-18]

In many vertebrate organisms, defects in cilia formation are the result of genetic pathologies such as autosomal recessive polycystic kidney disease[19-22] and Bardet-Biedl syndrome.[23-29] In *C. elegans*, the orthologs of these proteins maintain their function as necessary components in the generation and maintenance of sensory cilia associated with ciliated sensory neurons, but, however, do not cause severe dysfunction within the organism under laboratory conditions. Nevertheless, research into genes associated with IFT in *C. elegans* can provide insight into their human orthologs that have pathogenic attributes. IFT genes in *C. elegans* have been characterized previously, and mutants of these genes present with truncated cilia that do not reach the environment through the cuticle pore. Without exposure to the environment, they are incapable of absorbing a fluorescent lipophilic dye DiI, when immersed in it, into six pairs of amphid sensory cilia (ASK, ADL, ASI, ADF, ASH, and ASJ) and two pairs of phasmid sensory cilia (PHA, PHB). This results in what is known as a dye filling defective (Dyf) phenotype.[30,31] Here, through a variety of genetic techniques, we attempt to characterize two ethyl methanesulfonate (EMS) mutagen generated Dyf strains with unknown genetic lesions, WX737 *dyf-3(og022)*IV and PK841 *dyf-15(pk841)*V, as containing novel IFT genes.

II. Materials and Methods

Strains

Worms were grown on NGM plates seeded with *E. coli* strain OP50 at ~20°C (room temperature) using standard methods.[32] Wild-type strains used in this work are the Bristol (N2) and Hawaiian (CB4856) isolates. In addition, the mutations *dyf-3(og022)*IV and *dyf-15(pk841)*V were used in this work.

Dye-filling assay

Dye-filling assays were performed as described.[33] Worms were grown up using standard methods, washed off with M9 buffer into a microcentrifuge tube, and then washed with M9 at least three times. From here, 100 µl of the worm pellet was transferred to one well of a 250 µl x 8 polypropylene PCR strip. Another 100 µl of the remaining M9 solution was then subsequently transferred to the same well. This serves mainly to dilute the high concentration of worms originally transferred, which will facilitate the exposure of the worms to the dye. At this point 2 µl of DiI solution (Invitrogen) was added to this 200 µl worm solution, and the PCR strip was capped, taking care to turn the tubes upside down a few times to ensure even distribution of the dye solution. In addition, the PCR strip was wrapped in aluminum foil in order to limit exposure to ambient light. This mixture was then allowed to incubate for about 1 hour at room temperature while rotating on a vertical rotator. After incubation, the worms were washed at least three additional times with M9 and then plated on NGM plates free of bacteria. Bacteria can often autofluoresce both on the plate and in the worm gut, and plating on non-seeded media can aid in immediate scoring of Dyf animals. Observation

of dye-filled animals was conducted with a Zeis Stemi SV6 fluorescence microscope using a RITC filter.

Implementation of SNPs

All subsequent SNPs were analyzed and chosen using both the Wormbase website and the Washington University of St. Louis Medical School: *C. elegans* Single Nucleotide Polymorphism Database.

Bulk Segregant Analysis (BSA)

CB4856 is a geographically isolated strain of *C. elegans* that contains over 6000 SNPs that differentiate it genetically from the N2 Bristol strain. These differences in genotype can sometimes alter restriction enzyme cutting sites, creating a snipSNP that is detected as a RFLP after gel electrophoresis. These snipSNPs can then be used to trace parental genotypes for mapping purposes or to assess chromosomal linkage using 4 SNP markers on each chromosome, equally spaced from each other in what is known as BSA.[34]

In BSA, the Dyf strains of interest (mutagenized from N2 background) can be crossed with the marker strain, the Hawaiian isolate CB4856, to form an F1 population. The F1 population is then dye-filled as described[33] and 25-30 phenotypically WT heterozygotes are picked to create a new population, taking care to only to pick virgin hermaphrodites. Virgin animals can be determined by the absence of a copulatory plug, which appears as a mass over the vulva that often times will fluoresce under the UV scope. These virgin, hermaphroditic F1s are then allowed to recombine and generate an

F2 population. This F2 population is again dye-filled as described.[33] Two separate bulked lysates were formed from groups of 40-50 phenotypically WT or mutant (Dyf) F2 young adults, respectively.

To perform the analysis, separate PCR is performed using Taq DNA polymerase (New England Biolabs) on the two bulked lysates to amplify the selected snipSNPs using the primers described (Figure 1) and each separate product was digested using DraI. Subsequent analysis of these WT and mutant (Dyf) snipSNP digests via gel electrophoresis allows, given the expected RFLP band sizes for each genotype (Figure 1), determination of the genotype of the worm at each position involved in the BSA, be it N2, CB4856, or heterozygous (bands of both genotypes). Because the WT lysate has no associated linkage, random recombination is expected, and therefore the genotype should be heterozygous at every position on each chromosome. However, the mutant (Dyf) lysate should exhibit linkage around the genetic lesion, showing an appreciable bias of N2 genotype, compared to the WT, somewhere within the genome. Because a rough snipSNP map is used in the BSA, i.e. 4 snipSNPs per chromosome, this method will allow us to assess chromosomal linkage by observing at which snipSNP(s) there is a bias towards the N2 genotype in the mutant (Dyf) lysate.

snipSNP Mapping

Further genetic mapping of WX737 and PK841 was performed by the snipSNP method (Figure 2).[34] Standard molecular biological manipulations were performed as described.[35] Setting up the snipSNP mapping is similar to BSA, except instead of selecting populations of F2 WT and mutant (Dyf) animals, only individual F2 mutant

(Dyf) recombinant animals are selected, again taking care to only select virgin hermaphrodites. These individual mutant (Dyf) recombinant animals are segregated onto their own growth plates and allowed to produce their own populations of F3s. It is easiest to pick sets of 96 mutant (Dyf) animals, as it will facilitate subsequent lysis. Once a sizable population has grown up on a plate, the worms are washed into materials provided in the DNeasy 96 Blood and Tissue Kit (Qiagen). All lysis and wash buffer steps were performed as described, but a homemade setup was used for all centrifugations. These sets of 96 individual mutant (Dyf) recombinant strain DNA samples can then be used with a higher density snipSNP map. Eleven snipSNPs on chromosome IV were used in the mapping of 192 WX737 recombinant strains (Figure 3), and nine snipSNPs on chromosome V were used in the mapping of 288 recombinant PK841 strains (Figure 4). In a manner similar to the BSA snipSNP analysis, regions around the snipSNPs were amplified via PCR using Taq DNA polymerase (New England Biolabs) with the primers described and were digested using the enzymes described (Figures 3 and 4). Again, similar to BSA, the PCR'd and digested SNPs for each mutant (Dyf) recombinant strain are analyzed via gel electrophoresis and each SNP position can be genotyped as N2, CB4856, or heterozygous using the expected RFLP sizes described (Figures 3 and 4).

Sequencing of Candidate Gene *dyf-3*

The *dyf-3* gene of WX737 was amplified using Taq DNA polymerase (New England Biolabs) and the primers described (Figure 5). Bands of the 2938bp expected length were excised after gel electrophoresis and purified with a Qiaquick Gel Extraction

Kit (Qiagen). These *dyf-3* PCR fragments were then cloned into TOPO® vectors and transformed into DH5-T1R *E. coli* using a TOPO® TA Cloning Kit for Sequencing with One Shot® MAX Efficiency™ DH5-T1R E. coli Kit (Invitrogen) and the ascribed protocol. Transformed DH5-T1R *E. coli* were plated onto LB Kan plates and allowed to grow up overnight at 37°C. Individual colonies were picked and grown up overnight at 37°C in LB Kan cultures. TOPO® /*dyf-3* plasmids were harvested from the cultures using a Qiaquick Miniprep Kit (Qiagen). TOPO® /*dyf-3* plasmids were then verified by a diagnostic digest using EcoRI and analyzed by gel electrophoresis, observing for the expected bands of 3950bp (TOPO®) and 2938bp (*dyf-3*). TOPO® /*dyf-3* was sequenced using the described primers (Figure 5) by MWG-Biotech Inc.

RNA Isolation of Strains

To obtain whole genome RNA from both N2 and WX737 animals, 20 plates of each strain were chunked and allowed to grow up to maturity. Plates for each strain were then washed into separate 50ml conical tubes, pelleted, aspirated, and stored at -80°C. Portions of frozen worm pellets were added to a mortar and pestle and ground over ice until worm bodies had been reasonably crushed and dissolved. Subsequent RNA preparations were performed using the RNeasy Mini Kit (Qiagen) and the ascribed protocol. After elution of the RNA samples, 1µl of RNasin (Promega) was added to each, N2 and WX737, to aid in preservation. Samples were then frozen at -80°C for storage and subsequent use. Samples were analyzed by formaldehyde gel electrophoresis for qualitative confirmation of RNA presence.

RT-PCR of Strains

In order to obtain cDNA from our N2 and WX737 RNA samples, an Access RT-PCR System (Promega) was used with the primers as described (Figure 6). cDNA was analyzed by gel electrophoresis and the N2 and WX737 N2.Rev bands were excised and purified with a Qiaquick Gel Extraction Kit (Qiagen). These N2.Rev bands were then cloned into separate TOPO® vectors and transformed into DH5-T1R *E. coli* using a TOPO® TA Cloning Kit for Sequencing with One Shot® MAX Efficiency™ DH5-T1R E. coli Kit (Invitrogen) and the ascribed protocol. Transformed DH5-T1R *E. coli* were plated onto LB Kan plates and allowed to grow up overnight at 37°C. Individual colonies were picked and grown up overnight at 37°C in LB Kan cultures. The two TOPO® /N2.Rev plasmids were harvested from the cultures using a Qiaquick Miniprep Kit (Qiagen). The two TOPO® /N2.Rev plasmids were then verified by a diagnostic digest using EcoRI and analysis by gel electrophoresis, observing for the expected bands of 3950bp (TOPO®) and 786bp (N2.Rev bands). The two TOPO® /N2.Rev plasmids were then sequenced using the vector T3 and T7 primer sites by MWG-Biotech Inc.

Construction *dyf-3* Rescue Construct

A *dyf-3* rescue construct was assembled by 8 separate PCR amplifications of WT *dyf-3* off of the CO4C3 cosmid using Taq DNA polymerase (New England Biolabs) and the primers described (Figure 7). These 8 separate amplifications were then combined together and purified using a PCR Cleanup Kit (Qiagen). Germline transformation of WX737 *dyf-3(og022)*IV was performed as described.[36] WT *dyf-3* PCR (10ng/µl) product was coinjected with the pRF4 selectable marker plasmid which contains *rol-6(su1006)* at

50 ng/µl. Animals exhibiting the ROL phenotype were selected for and allowed to self. F1s were dye-filled as described[33] using DiI to confirm rescue of the WT phenotype.

III. Results

The *dyf-3* and *dyf-15* genes affect cilia morphogenesis

dyf-3 mutants have been previously shown to exhibit defects in the uptake of a fluorescent dye DiI in six pairs of ciliated sensory neurons (ASK, ADL, ASI, ADF, ASH, ASJ) when compared to the wild-type N2 (Figure 8). Along with this Dyf phenotype, *dyf-3* mutants possess defects in the function of some sets of amphid neurons, including chemotaxis to NH_4Cl and osmotic avoidance.[31] Previous work using *gfp* gene expression under the control of a promoter specific for a single or group of sensory neurons in wild-type and *dyf-3(m185)* animals has shown truncated cilia and abnormal posterior projections in ADF, AWB, and ASE neurons in the mutant.[37]

dyf-15(pk841) mutants observed in this study exhibited a partially penetrant dye-filling-defective phenotype in amphid sensory cilia (data not shown) but those animals that were dye-filling-defective were similar in nature to that of the Dyf phenotype in amphid sensory cilia of *dyf-3* mutants.

Identification of chromosomal linkage in strains WX737 and PK481

Bulk Segregant Analysis (BSA) was used to assess chromosomal linkage for the genetic lesions affecting strains WX737 and PK841 according to the Materials and Methods. Because it is known that WT lysate animals have not recombined the genetic lesion, it can be assumed that the net genetic profile of this bulked lysate will be heterozygous because there is no bias for linkage on any of the chromosomes. In the mutant (Dyf) lysate population, the “rescue” of the Dyf phenotype indicates that the animals selected have had a recombination event that has created a homozygous area

around the genetic lesion. Therefore, because the mutant was N2-derived, a bias for the homozygous N2 genotype in the area around the genetic lesion should be observed, indicating linkage for the allele in question.

In the BSA for strain WX737 (Figure 9), a bias for the N2 genotype in the Mutant lanes at positions IV:-4cM and IV:1cM can be observed when compared to the WT lanes, indicating linkage for the *og022* allele on chromosome IV. All other chromosomes exhibited no linkage when subjected to BSA analysis (data for chromosomes I, II, V, and X not shown).

In the BSA for strain PK841 (Figure 10), there is a noticeable bias for the N2 genotype in the Mutant lanes at positions V:-7cM and V:5cM when compared to the WT lanes, indicating a linkage for the *pk841* allele on chromosome V. All other chromosomes exhibited no linkage when subjected to BSA analysis (data for chromosomes I, II, and III not shown).

Genetic mapping of strains WX737 and PK841

The alleles *og022* and *pk841* were mapped using the snipSNP method by using single-nucleotide polymorphisms between the N2-derived mutant strains and the CB4856 strain as described in the Materials and Methods. When this analysis is done across large sets of mutant (Dyf) recombinant strains, a large-scale genetic mosaic begins to form. Because the genetic lesions of interest are within an N2 background (i.e., mutants are N2 derived), patches of homozygous N2 genotype that are substantiated through multiple strains indicate a possible interval in which the genetic lesion may lie. Given sufficient

shortening of this interval using higher density snipSNP maps allows for eventual identification and sequencing of candidate genes within the interval.

It is important to note that for the ease of visualization when discussing allele location during snipSNP mapping, the chromosome is thought of in a horizontal fashion where all negative genetic positions are considered to be *to the left* of positive genetic positions. That is, given any point on a chromosome, when a position *to the left* is discussed, a position with a more negative genetic position number is meant, and when a point *to the right* is discussed, a position with a more positive genetic position number is meant.

The *og022* allele of strain WX737 was mapped to a small region between IV:-4.56 and IV:-4.17cM, a 0.39cM interval (Figure 11). Of particular note here are strains B5 and C7. In recombinant strain B5, it is observed that snipSNPs at IV:-7cM and IV:-4.56cM exhibited the heterozygous genotype, whereas all other positions at IV:-4.17cM and to the right exhibited the N2 genotype, indicating that, in our linear representation, the genetic lesion of interest is located somewhere to the right of IV:-4.56cM. Looking at recombinant strain C7, the opposite is observed; snipSNPs at IV:-4.56cM and IV:-7cM exhibited the N2 genotype, while positions at IV:-4.17 and to the right exhibited the heterozygous genotype, indicating that the genetic lesion of interest is located somewhere to the left of IV:-4.17cM. When the genetic profiles of these two strains are compared, it becomes apparent that the *og022* allele therefore lies between positions IV:-4.56cM and IV:-4.17cM, a conclusion that is substantiated by the other mapped strains (Figure 11).

The *pk841* allele of strain PK841 was mapped to a region between V:2.99cM and V:5.83cM, a 2.84cM interval (Figure 12), also using the snipSNP mapping method. Of particular note are strains D7 and E4. In recombinant strain D7, it can be observed that snipSNPs at V:5.83cM and to the right exhibited the heterozygous genotype, while positions at V:4.00cM and to the left showed the N2 genotype, indicating that the genetic lesion of interest is somewhere to the left of V:5.83cM. For recombinant strain E4, it can be observed that snipSNPs at positions V:2.99 and to the left showed the heterozygous genotype, while positions at V:4.00cM and to the right exhibited the N2 genotype, indicating that our genetic lesion of interest is somewhere to the right of V:2.99cM. When this information is collated, it can be seen that the *pk841* allele must lie somewhere between positions V:2.99cM and V:5.83cM, which is supported by the other mapped strains of interest (Figure 12). Because the causal gene for PK841 was not located in this study, it was given the temporary experimental gene name *dyf-15(pk841)*.

Identification of *dyf-3(og022)*

It was determined using the Wormbase gene database that there were 14 known genes within our experimental interval for allele *og022* between IV:-4.56cM and IV:-4.17cM.[38] Of particular note was the known Dyf gene *dyf-3*, and it was hypothesized that allele *og022* might be located within this ORF. The *dyf-3* gene of strain WX737 was then sequenced, and a C to T mutation was found on the positive strand in the first base pair after the third exon of the CO4C3.5b splice variant (Figure 13).

The *og022* allele affects proper spliceosome cycling

The *dyf-3* gene runs 3'→5' with the start codon ATG on the negative strand. The CO4C3.5b splice variant has nine exonic regions, with intronic regions between each. Because *og022* is located in the first base pair of the third intronic sequence of *dyf-3* CO4C3.5b, it was theorized that the mutation could alter some conserved portion of the exon/intron boundary, thereby causing defects in mRNA splicing. The conserved eukaryotic 5' splice-site (5'ss) sequence across most invertebrate organisms is NAG|GTAAGT where "|" represents the specific 5'ss, i.e. the exon-intron boundary.[39] Therefore, the *og022* mutation alters this conserved sequence at the first guanine residue of the intronic sequence, and should alter the ability of the spliceosome to create properly spliced mature mRNA of *dyf-3*.

In order to observe the potential affect of the *og022* allele on the splicing of *dyf-3* mRNA, reverse-transcription (RT)-PCR of *dyf-3* in N2 and WX737 animals was performed (Figure 14). As can be seen, when using primers encompassing the entirety of the first four exons of *dyf-3*, we notice a difference in band length in the N2 and WX737 cDNA amplicons. Also, when using primers within the third intronic sequence, the presence of cDNA when amplifying off of WX737 mRNA is observed, but not with N2. When the cDNA of *dyf-3(og022)* was sequenced, it was confirmed that the entire third intron had been spliced into the mature *dyf-3* mRNA (Figure 15) as a result of the defect in the 5'ss created by the *og022* allele. This newly spliced-in intron codes for a premature stop-codon, thereby severely truncating DYF-3 to include only the first three of its nine exons.

Phenotypic rescue of *dyf-3(og022)*

As previously mentioned, *dyf-3(og022)* animals fail to uptake fluorescent DiI in amphid sensory neurons. A rescue construct of the WT *dyf-3* gene containing about 800bp of 5'UTR and about 200bp of 3'UTR was created and injected as detailed in the Materials and Methods. This WT copy of the gene was able to fully re-establish the WT dye-filling phenotype of the worm (Figure 16).

IV. Discussion

dyf-3 is expressed in a subset of sensory neurons

It has been shown that *dyf-3*::GFP fusion expression can be observed in eight pairs of amphid sensory neurons (ASE, ADF, ASG, ASH, ASJ, ASK, ASI and ADL), six inner labial neurons (IL2s) and two pairs of phasmid neurons (PHA, PHB). All of these neurons have chemosensory properties due to ciliated endings that are exposed to the outside environment. The functional DYF-3::GFP protein was observed to be distributed uniformly in cell bodies, dendrites and axons. In addition, it has been shown by expressing *dyf-3* in all sensory neurons using an *osm-6* promoter that the same selective group of neurons would dye-fill with DiI as in the wild-type background. Therefore, it has been concluded that the DYF-3 protein is necessary but not sufficient for the uptake of a fluorescent dye, and *dyf-3* acts cell-autonomously with respect to dye uptake.[37]

The *og022* allele alters the 5' splice-site and disrupts spliceosome cycling

Because the *og022* allele is positioned at the first base pair of the third intronic sequence of *dyf-3*, it effects the conserved sequence of the 5'ss for this intron. This mutation therefore disrupts the binding of the U1 snRNP, which is the first step of the spliceosome cycle. Without U1, the cycle is then unable to designate the 5'ss to be used and also fails to recruit the U4/U5/U6 snRNP complex in downstream steps of the splicing process (Figure 17).[40] The end result is a failure of the spliceosome to remove the third intron of *dyf-3* pre-mRNA, which therefore causes the intron to be included in the mature mRNA. This new segment of mature mRNA codes for a premature stop codon, which, upon translation, will cause DYF-3 to be severely truncated.

Expression of *dyf-3* is regulated by the DAF-19 transcription factor

In *C. elegans*, all known IFT complex B genes are regulated by a regulatory factor for X box (RFX) family transcription factor DAF-19, and contain a DAF-19 recognition sequence, called X box, in their upstream genomic regions.[21,41,42] As previously described, the cilia of some sensory neurons in *dyf-3* mutants are truncated and have abnormal posterior projections which are similar in nature to many IFT complex B mutants.[30] In addition, it was noted previously, and again in this study, that 75bp to 88bp upstream of the start codon of *dyf-3* CO4C3.5b there is an X box-like sequence (GTTTCT AT GGGAAC).[37] In this sequence, 13 of the 14 base pairs are identical with the consensus *C. elegans* X box sequence (GTTNCC AT GGNAAC).[41] Previous work has also shown that *dyf-3::gfp* expression levels are greatly reduced in *daf-19* mutants, such as *daf-19(m86)*.[37] Because of the similarities in cilium structure defects between *dyf-3* and IFT complex B mutants, and the existence of an X box-like recognition sequence indicating that the gene is regulated by DAF-19, it is has been suggested that *dyf-3* acts as a component of the IFT system.[37]

***dyf-3(og022)* and *dyf-15(pk841)* function for cilia morphogenesis**

In order to analyze genes affecting cilia morphogenesis, our lab investigated two strains, WX737 and PK841, which contained mutations that produce defective sensory cilia. Although the causal gene for the *pk841* allele of strain PK841 was not fully characterized within this study, the interval in which the genetic lesion lies has been narrowed down to an area between V:2.99cM and V:5.83cM.

The *dyf-3* gene has been shown to encode a protein necessary for cilia morphogenesis, which is a critical process in order for *C. elegans* to receive external cues and stimuli. It has been shown that *dyf-3* animals exhibit defects in chemotaxis towards several environmental factors, and fail to uptake fluorescent DiI through their ciliated sensory neurons.[37] DYF-3 has also been shown to be homologous to CLUAP1 (Clusterin Associated Protein 1) homologs in humans and zebra fish, although these homologies are largely based on informatics predictions.[38] Unfortunately, although many IFT related proteins in various organisms have been previously characterized, database searches have not produced an IFT associated protein that is homologous to DYF-3.[37]

It has been suggested, and this investigation supports, that DYF-3 is involved in IFT complex B based on morphological similarities in the amphid cilia of *dyf-3* and IFT complex B mutants[30] and the presence of an X box like regulatory sequence 75bp to 88bp upstream of the *dyf-3* CO4C3.5b start codon. This positioning of the sequence indicates that expression of *dyf-3* is likely regulated by DAF-19, much like other IFT complex B genes.

It is important to note, however, that previous studies have observed differences between *dyf-3* and known IFT complex B genes. While *dyf-3::gfp* expression has been visualized in the cell bodies, dendrites, and axons of a select number of ciliated sensory neurons, most known IFT complex B genes are expressed in all neurons and GFP fusions can be visualized only in cilia and cell bodies.[22, 37, 43, 44] In addition, attempts to observe expression using a *dyf-3* promoter::GFP have proved to be unsuccessful, suggesting that another genomic region, possibly a 3' untranslational region, or additional regulators other than DAF-19, are necessary for *dyf-3* expression.[37]

All of this information has lead to the conclusion that DYF-3 most likely acts in the IFT system of selective sensory neurons, and may function to provide specific modifications for these sensory endings. Also, previous observations that DYF-3::GFP is distributed widely in cell bodies, dendrites and axons of the neurons in which it is expressed suggests that DYF-3 plays other roles than just as a component of the IFT system, such as interactions with OSM-12/BBS-7.[37]

Directions for future work

The next step for this project would be to shorten the experimental interval for *dyf-15(pk841)* using higher density snipSNP mapping in order to find an appropriate amount of candidate genes to begin sequencing. This will allow for the identification of the causal gene in which the *pk841* allele is located. Known Dyf genes located within the experimental interval of V:2.99cM and V:5.83cM are *che-11*, *dyf-4*, and *odr-3*. If mating with PK841 can be accomplished, complementation tests with these genes can be performed in lieu of large-scale sequencing.

Subsequent research into *dyf-3(og022)* should primarily focus on the proteomic aspects of DYF-3. Investigation into the potential adverse effects of the severely truncated DYF-3 protein *in vivo,* and its influence on levels DYF-3 production could yield insight into how egregiously malformed proteins are handled in *C. elegans*. Also, observation of time-lapse confocal microscopy to try and visualize the movement of DYF-3::GFP and its possible association with GFP tagged IFT complex rafts may allow for the elucidation of the responsibilities and interactions of DYF-3 with other components of the IFT system.

snipSNP Position	Cosmid/YAC	N2 Digest	CB4856 Digest	Sequences
I:-27cM	F56C11	350bp, 150bp	500bp	**For:** ATGCCAGTGATAAGGAACGG **Rev:** TCACATCCCTTGTCGATGAA
I:-6cM	W03D8	400bp, 130bp	530bp	**For:** GTTTTCACTTTTGCCGGTGT **Rev:** TGAAGGCGCATATACAGCAG
I:-1cM	D1007	321bp, 134bp, 38bp	455bp, 38bp	**For:** AAAATATCAGGAAAGAGTTTCGG **Rev:** TTTAAAGATTAAGGGTGGAGCG
I:12cM	F58D5	450bp	300bp, 150bp	**For:** TCCTGGATAATCCCCAAAAA **Rev:** CCCTGCCATTGATCTTGTTT
II:-16cM	T01D1	265bp, 109bp	374bp	**For:** CCGAATTTTCAAATGGATGC **Rev:** CCATTGGAATTGCACACAAA
II:-5cM	F54D10	516bp	387bp, 129bp	**For:** TTGTGAGCTTATATCTCAGTTGTCG **Rev:** AGATTTGGTTAGAAATATCACCGC
II:1cM	T24B8	372bp, 122bp	494bp	**For:** TCAAAAACTTACAATCAATCGTCG **Rev:** CCAGAAAATCTGCACAGAAGG
II:14cM	F15D4	541bp	408bp, 133bp	**For:** TTTCAATTTCTTTCCCATTTTCC **Rev:** AAAAACACAAAGTTCAAAAACCC
III:-13cM	Y71H2B	367bp, 105bp	473bp	**For:** GAGGAACCAAATCTGGCGTA **Rev:** TGAAAACTTGGAAAATCGGTG
III:-1cM	F56C9	485bp	335bp, 150bp	**For:** AAAAATACATGTCTACACAACCCG **Rev:** TTTCTTATCACTGTGCAGTCTTACC
III:4cM	Y39A1A	335bp, 171bp	526bp	**For:** AGCGTTAAAGTATCGGTTATTTCG **Rev:** TAAATTCATTTCAAACAATCGAGC
III:10cM	Y41C4A	339bp, 153bp	492bp	**For:** ATCAAGTTTCTGATTGCTCTTTCC **Rev:** AAAAACGTGATTTTTCAATTTTGC
IV:-15cM	Y41D4B	378bp, 155bp	533bp	**For:** CACACACAAATACATCCCAATACC **Rev:** CATTTAGAGAATTACTGTAGCTTTCGC
IV:-7cM	Y54G2A	498bp	250bp, 248bp	**For:** ACTCGGCATCCTCACGC **Rev:** GTTGAAAATTTTTTCATAGCTATCATC
IV:1cM	E03H12	375bp	297bp, 78bp	**For:** AAAATGGGAAGCGTACCAAA **Rev:** TGCTTGTAGCGTTTCCAAGA
IV:22cM	Y105C5B	238bp, 113bp, 78bp, 48bp	318bp, 113bp, 48bp	**For:** TCGAATTGTTGTGTTTCTTTTGA **Rev:** TTCCAATTTTCTCGGTTTGG
V:-19cM	F36H9	331bp, 84bp, 79bp	410bp, 84bp	**For:** TTTCGGAAAATTGCGACTGT **Rev:** CGCGTTTTGGAGAATTGTTT
V:-7cM	Y61A9LA	454bp	307bp, 147bp	**For:** GAGATTCTAGAGAAATGGACACCC **Rev:** AAAAATCGACTACACCACTTTTAGC
V:5cM	R10D12	500bp	348bp, 152bp	**For:** CAAATTAAATATTTCTCAAAGTTTCGG **Rev:** ACATAAGCGCCATAACAAGTCG
V:22cM	Y17D7B	324bp, 164bp	488bp	**For:** GAAATTCAAATTTTTGAGAAACCC **Rev:** TTCAGACCATTTTTAGAATATTCAGG
X:-15cM	F49H12	540bp	320bp, 220bp	**For:** ATATGTGAGTTTACCATCACTGGG **Rev:** ACGTTTTGAAAAATTTGGTTGC
X:-8cM	ZK470	452bp, 78bp	350bp, 102bp, 78bp	**For:** ACCCATTGCTACTTTTTCCTATCC **Rev:** GAAGTTGCACTCTTTCTCCTTCC
X:2cM	C05C9	444bp, 96bp	540bp	**For:** ACACTAGAATCTCCACACCTCC **Rev:** CGCACTGACTTTTTTCCAGC
X:12cM	F46G10	320bp, 191bp, 34bp	546bp	**For:** ACTGTTTACCGCGTCTTCTGC **Rev:** CCGTGTATATAAGAAAATGTGTTCG

Figure 1. BSA primers used with associated cosmid/YAC locations and RFLPs as described in Materials and Methods. All digests performed with DraI.

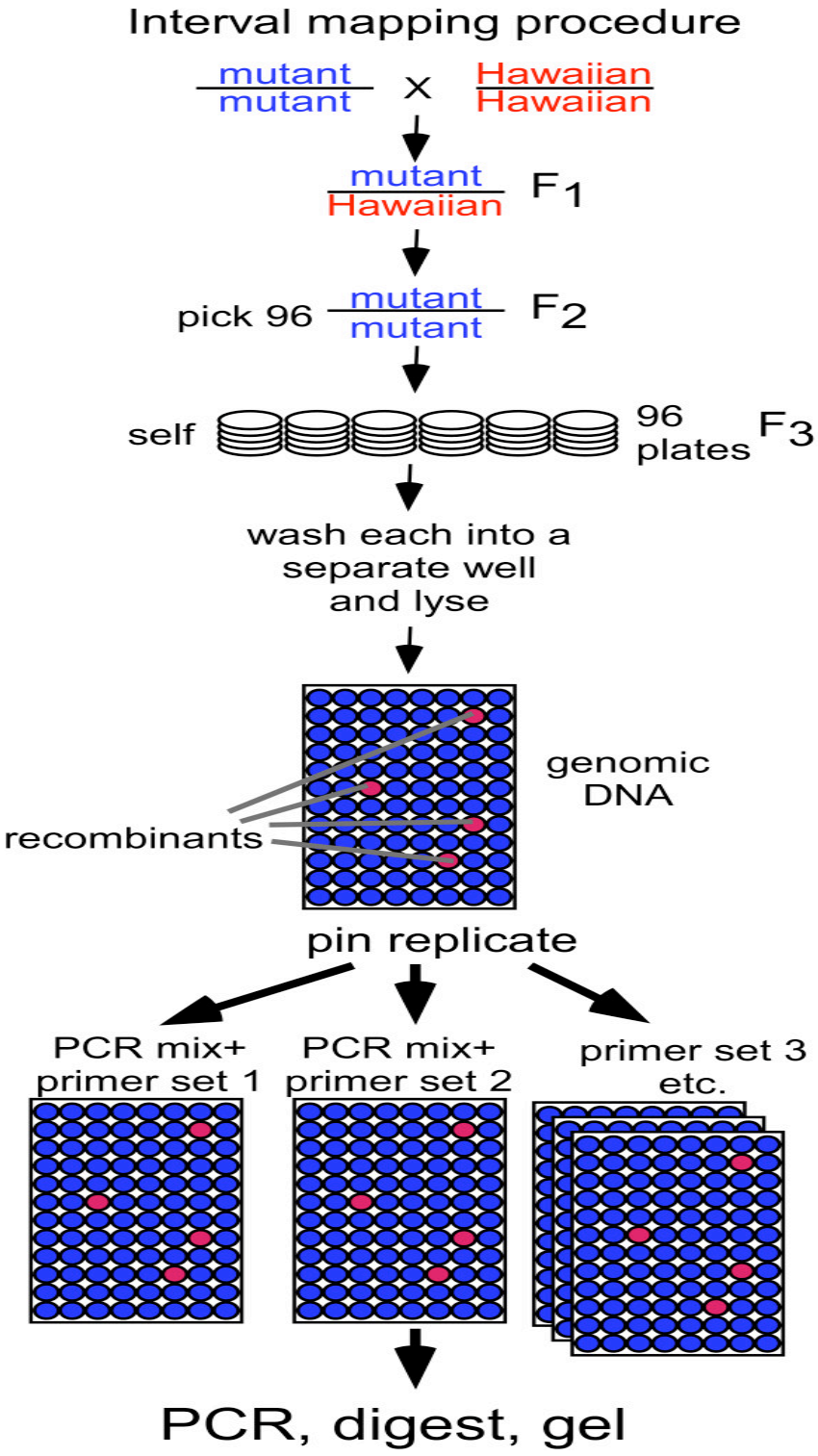

Figure 2. A summary of the snipSNP method as described in the Materials and Methods.

snipSNP Position	Cosmid or YAC	Enzyme	N2 Digest	CB4856 Digest	Primer Sequences
IV:-15cM	Y41D4B	DraI	378bp, 155bp	533bp	**For:** CACACACAAATACATCCCAATACC **Rev:** CATTTAGAGAATTACTGTAGCTTTCGC
IV:-7cM	Y54G2A	DraI	498bp	250bp, 248bp	**For:** ACTCGGCATCCTCACGC **Rev:** GTTGAAAATTTTTTCATAGCTATCATC
IV:-4.56cM	F42A6	DraI	296bp, 122bp	418bp	**For:** TGCTGAAATATTGGAAAATTGAGG **Rev:** TTATATCGTCGAGGAGGTTAGAGG
IV:-4.17cM	C04C3	N/A	N/A	N/A	**For:** AGACCAACGATTATCACTCTG **Amp Prim** **Rev:** ATCCCAGCTATGAATATAACG **Amp Prim** **For:** ATCTCCATTTTTCAACTTTGC **Seq Prim** **Rev:** TGAACAGGTGATACTAAATTTC **Seq Prim**
IV:-3.76cM	C09G12	N/A	N/A	N/A	**For:** CAAGATTCTCACATTCCGTCTG **Amp Prim** **Rev:** GTTCGCTCAAGAACCAAATG **Amp Prim** **For:** GATGAGCGGTGTTGCGTAG **Seq Prim** **Rev:** CGTCATCACCCAAGTCTTCC **Seq Prim**
IV:-3.64cM	C09G12	RsaI	164bp, 131bp, 30bp	295bp, 30bp	**For:** ATCCAGCTCAAAAGTGTGCG **Rev:** TGTCTACCGTATACCTGGAC
IV:-3.44cM	M57	NlaIII	398bp, 167bp, 19bp	295bp, 167bp, 103bp, 19bp	**For:** TCTCCCTAAAATACCCATGCAG **Rev:** TGGGATTGAATTTGCAATATAGG
IV:-3.33cM	B0212	AflIII	517bp	284bp, 233bp	**For:** TCCCTAAGCCAAGTGGTTTC **Rev:** AGAAGAAGCTATGGGAGTGCC
IV:-2.97cM	Y37E11AL	PstI	427bp	213bp, 209bp	**For:** TCCGCAGTTTTGACCAGAAG **Rev:** CCGCCCTTCTATGTGGAGTG
IV:-2.23cM	M02B7	NruI	302bp, 226bp	528bp	**For:** CTTGGAGTTGCCAAGAAGC **Rev:** TTAATTGGTGGAACTTTCGG
IV:~1cM	E03H12	DraI	375bp	297bp, 78bp	**For:** AAAATGGGAAGCGTACCAAA **Rev:** TGCTTGTAGCGTTTCCAAGA

Figure 3. WX737 *dyf-3(og022)*IV snipSNPs, primers, enzymes, and RFLPs used as described in Materials and Methods. Note: snipSNPs IV:-4.17cM and IV:-3.76cM are sequencing SNPs. Primers used to amplify the SNPs are labeled Amp Prim, while primers used to sequence the SNP are labeled Seq Prim.

Position	Cosmid or YAC	Enzyme	N2 Digest	CB4856 Digest	Primer Sequences
V:-17.64cM	F36H9	DraI	331bp, 84bp, 79bp	410bp, 84bp	**For:** TTTCGGAAAATTGCGACTGT **Rev:** CGCGTTTTGGAGAATTGTTT
V:-5.11cM	Y61A9LA	DraI	454bp	307bp, 147bp	**For:** GAGATTCTAGAGAAATGGACACCC **Rev:** AAAAATCGACTACACCACTTTTAGC
V:0.55cM	VC5	DraI	432bp, 79bp	297bp, 135bp, 79bp	**For:** AGAAATGATCCGATGAAAAAGC **Rev:** CCGATAGTGTTCATAGCATCCC
V:2.00cM	E02C12	AseI	355bp	289bp, 46bp	**For:** ATGCATAATGAGATGTGACTGG **Rev:** CAGACTCCCAAAATGCTCAG
V:2.99cM	T19B10	BsiHKAI	715bp	488bp, 227bp	**For:** CAACCTACTCTGCCTTTTGC **Rev:** TATTTCCCGCAATGCTCTCC
V:4.00cM	F55C5	TaqαI	128bp, 140bp, 191bp	268bp, 191bp	**For:** TGTTGTAGATGGACGGGCAG **Rev:** CAAACGCCTGCATCACTGAC
V:5.83cM	R10D12	DraI	500bp	348bp, 152bp	**For:** CAAATTAAATATTTCTCAAAGTTTCGG **Rev:** ACATAAGCGCCATAACAAGTCG
V:12.92cM	Y6G8	DraI	282bp, 205bp	487bp	**For:** CATTCATTTCACCTGTTGGTTG **Rev:** TCGGGAAGATAATCAAAATTCG
V:17.75cM	Y17D7B	DraI	324bp, 164bp	488bp	**For:** GAAATTCAAATTTTTGAGAAACCC **Rev:** TTCAGACCATTTTTAGAATATTCAGG

Figure 4. PK841 *dyf-15(pk841)*V snipSNPs, primers, enzymes, and RFLPs used as described in Materials and Methods.

(a)

Forward Primer Name	Sequence
dyf-3ForC	TTCCAGGTTATGGCTCAAGC
Reverse Primer Name	Sequence
dyf-3RevB	TCCTCTCGAAAAATGTGTGC

(b)

Sequencing Primer Name	Sequence
dyf-3SeqFor	TTTTTTGACGATCTCTAATTG
dyf-3SeqFor2	TATAATCCGCCTCGCTTCTC
dyf-3SeqFor3	TTACCTCATAAAGTTTCTTCAG
dyf-3SeqFor4	AGAAGTCCAAGCTTTTTACTG
dyf-3SeqFor5	AATTTTGGAGCATCAGGAG
dyf3-SeqRev	AGTCTTTGGGGTGTTTGCAG
dyf-3SeqRev2	AACTTTGGCCACTAACTTCC
dyf-3SeqRev3	AGGCAACAGTGCAGAACATC
dyf-3SeqRev4	AGAGCTCGACGAGAAGATAG
dyf-3SeqRev5	ACATGATGGGTGGTGATGC

Figure 5. Primers used for the (a) amplification of the 2938bp *dyf-3* gene and (b) sequencing of the amplicon in strain WX737.

Forward Primer Name	Sequence
rDyf3.Start.For2	ATGTCGTATCGTGAGCTGAG

Reverse Primer Name	Sequence	Band Length w/ rDyf3.Start.For2
Dyf3.both.Rev2	CTTCGTGTGCGTCAAGGTT	169bp (N2) 169bp (WX737)
Dyf3.N2.Rev1	CGTACTCGTCCATATACTGA	730bp (N2) 786bp (WX737)
Dyf3.dyf3.Rev2	CTTTTTCAGGCTGGTGGCCT	0bp (N2) 424bp (WX737

Figure 6. Primer sets used for RT-PCR amplifications of *dyf-3* (See Figure 15) and the expected amplicon sizes in N2 and WX737 *dyf-3(og022)*IV backgrounds. All reactions used the forward primer rDyf3.Start.For2 paired with a unique reverse primer.

Forward Primer Name	Sequence
dyf-3ForC	TTCCAGGTTATGGCTCAAGC
Reverse Primer Name	Sequence
dyf-3::RescueRev	ATAGCCTGATTTAGGGCGTC

Figure 7. Primers used to amplify the wild-type *dyf-3* rescue construct. This primer set will amplify *dyf-3* with 798bp of 5'UTR (gene-wise) and 208bp of 3'UTR (gene-wise) to produce a rescue construct 3543bp in size.

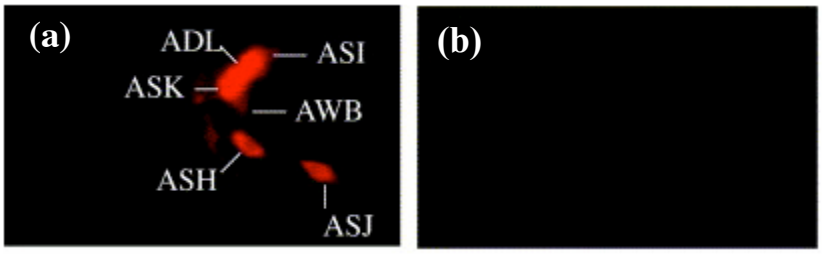

Figure 8. Cilium morphology of sensory neurons in the wild-type and mutant strains visualized by uptake of DiI as described in Materials and Methods. Anterior portion of the worm is to the left. Dye uptake is visualized in (a) WT and (b) WX737 *dyf-3(og022)* backgrounds.

Figure courtesy of:
Murayama, T., Toh, Y., Ohshima, Y., Koga, M. (2005). The dyf-3 gene encodes a novel protein required for sensory cilium formation in Caenorhabditis elegans. *Journal of Molecular Biology*, **346**, 677-687.

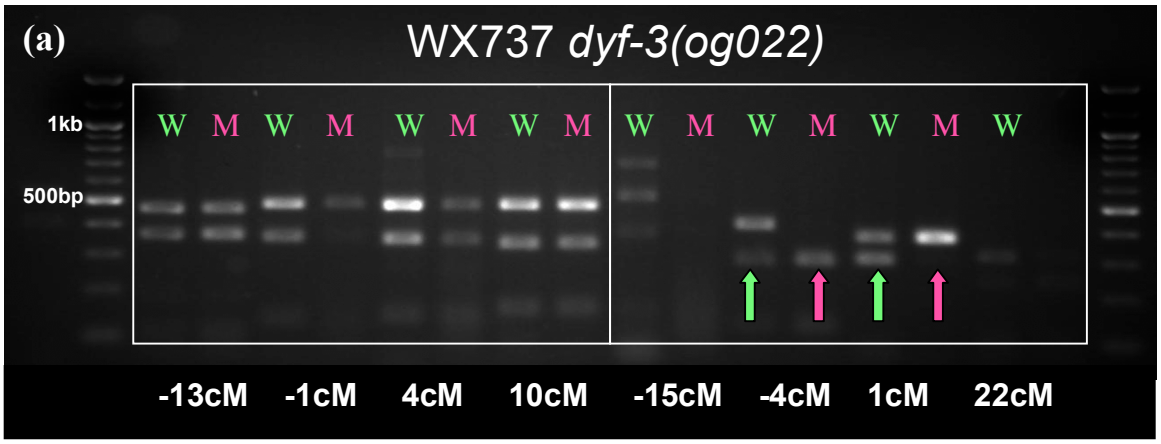

(b) RFLP Sizes on IV

Position	N2	CB4856
IV:-15	378, 155	533
IV: -4	296, 122	419
IV:1	375	297, 78
IV:22	238, 113, 78, 48	318, 113, 48

Figure 9. (a) Shows the BSA gel for strain WX737 on chromosome III and IV, with (b) the associated RFLP sizes at each position on chromosome IV for the two genotypes. Lanes in the BSA gel are alternating WT (W) and Mutant (M) populations, with a 100bp ladder (NEB) as a standard. As can be seen in panel illustrating chromosome III, W and M lanes at each position are identical, indicating a non-linkage associated recombination that presents a heterozygous genotype at each position. On the panel showing chromosome IV, a bias for the N2 genotype at positions IV:-4 and IV:1 can be observed.

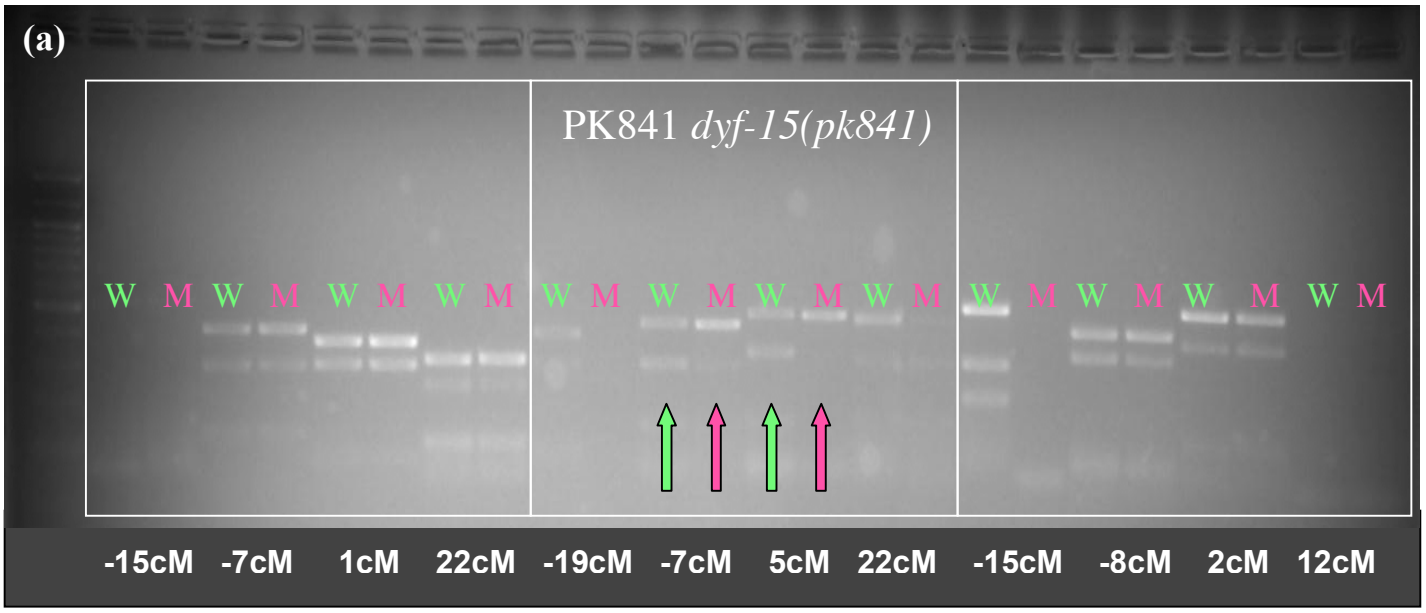

(b) RFLP Sizes on V

Position	N2	CB4856
V:-19	309, 84, 79	388, 84
V:-7	450	150, 300
V:5	500	350, 150
V:22	325, 160	485

Figure 10. (a) Shows the BSA gel for strain PK841 on chromosomes IV, V, and X with (b) the associated RFLP sizes at each position on chromosome V for the two genotypes. Lanes in the BSA gel are alternating WT (W) and Mutant (M) populations, with a 100bp ladder (NEB) as a standard. As can be seen in panels illustrating chromosomes IV and X, W and M lanes at each position are identical, indicating a non-linkage associated recombination that presents a heterozygous genotype at each position. On the panel showing chromosome V, a bias for the N2 genotype at positions V:-7 and V:5 can be observed.

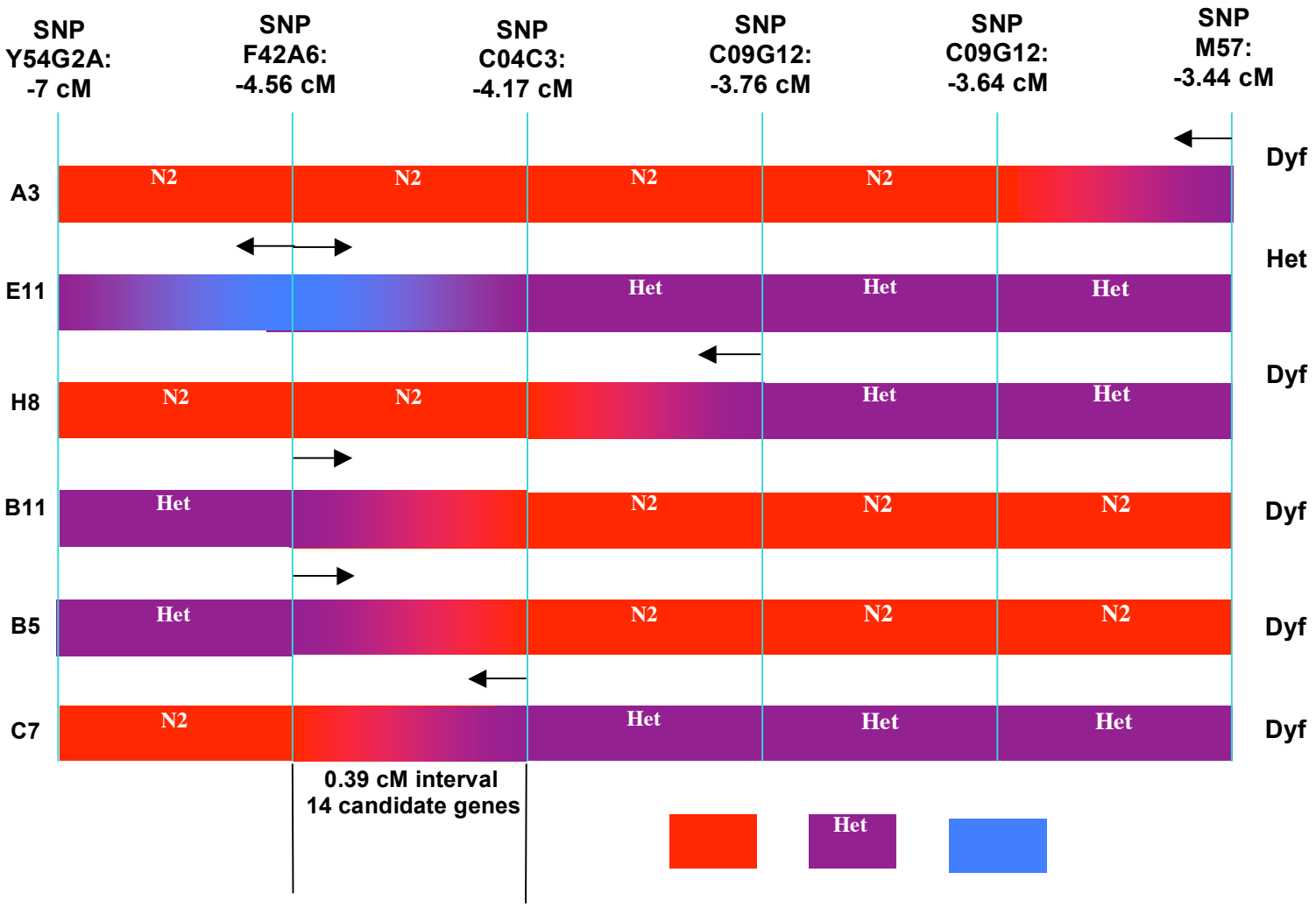

Figure 11. A graphical representation of six pertinent snipSNP mapping strains for WX737 *dyf-3(og022)*IV on chromosome IV. The phenotype of each strain is noted to the right. The genotype for each strain at the listed SNP positions is noted along the associated bar, and the arrows above each strain bar show the interval where snipSNP mapping has indicated the genetic lesion is located. For example, for strain H8, the genotype of the worm is N2 (mutant background) at all positions left of -3.76cM and heterozygous at all positions right of -3.76cM. The left facing arrow at this position indicates the genetic lesion is, according to this strain, located to the left of -3.76cM. Based on the these results, and corroborating data (not shown), the WX737 genetic lesion is located between IV:-4.17 and IV:-4.56.

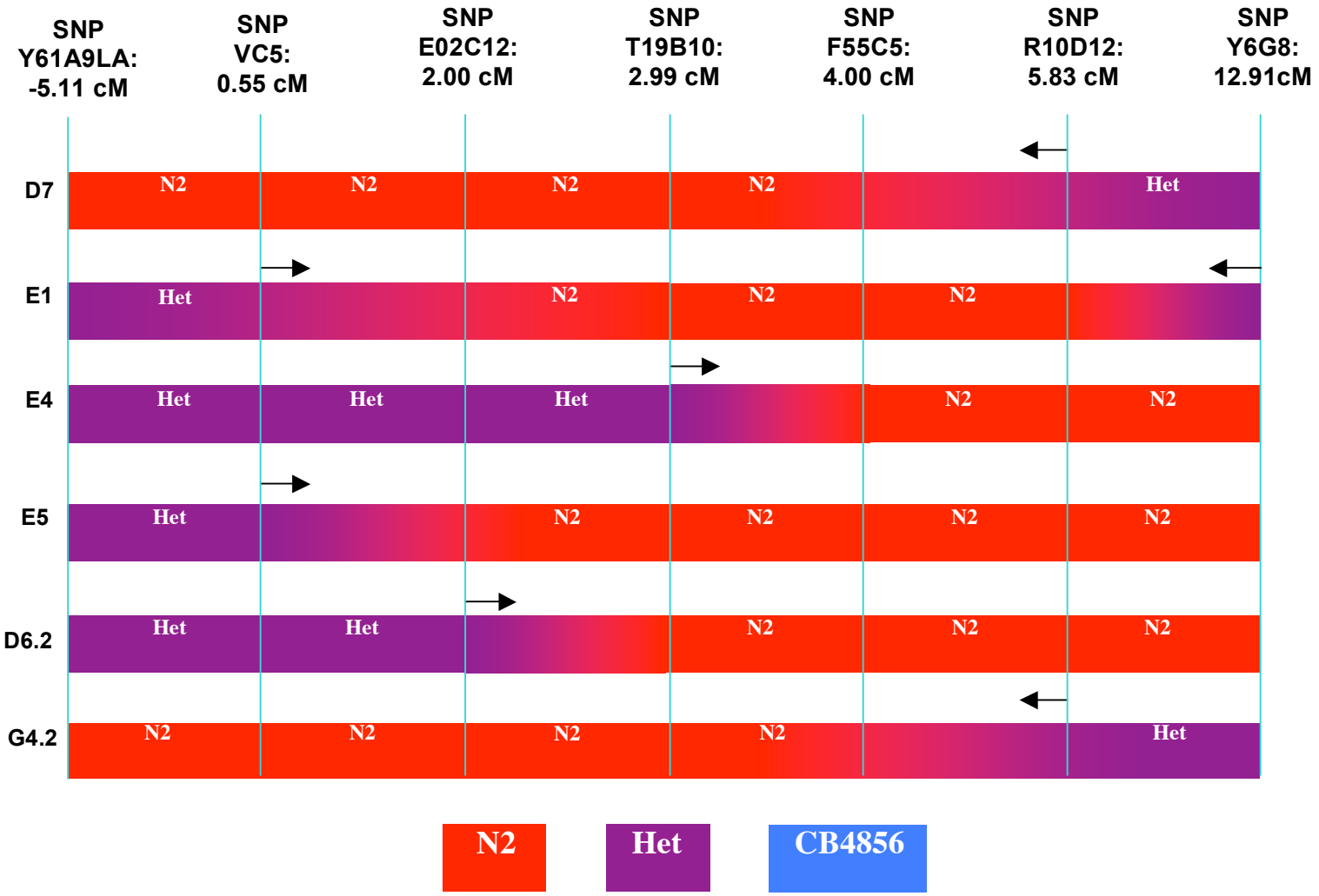

Figure 12. A graphical representation of six pertinent snipSNP mapping strains for PK841 *dyf-15(pk841)*V on chromosome V. All strains present phenotypically as Dyf. The genotype of each strain at the listed SNP positions is noted along the associated bar, and the arrows above each strain bar show the interval where snipSNP mapping has indicated the genetic lesion is located. For example, for strain E4, the genotype of the worm is heterozygous at all positions left of 2.99cM and N2 (Mut) at all positions right of 2.99cM. The right facing arrow at this position indicates the genetic lesion is, according to this strain, located to the right of 2.99cM.

(a)

```
Query:     1 GATGATAGCTGACGAGTGATTCGGACCTCCTGCATCTGAACTTTCGACAGTTTTTTCAGG 60
             ||||||||||||||||||||||||||||||||||||||||||||||||||||||||||||
Sbjct:  8358 GATGATAGCTGACGAGTGATTCGGACCTCCTGCATCTGAACTTTCGACAGTTTTTTCAGG 8417

Query:    61 CTTTTTCAGGCTGGTGGCCTGTGAGACCCATCTTCGACGAGAGCTTATTCTTGACTTGGG 120
             |||||||||||||||||||||||||||||| ||||||||||||||||||||||||||||
Sbjct:  8418 CTTTTTCAGGCTGGTGGCCTGTGAGACCCACCTTCGACGAGAGCTTATTCTTGACTTGGG 8477

Query:   121 TCCATTTTGGCGAGTTATCAGTGTTCGGGTCCTCTGCCTTGGCCTGGTAGAGGATCTTCA 180
             ||||||||||||||||||||||||||||||||||||||||||||||||||||||||||||
Sbjct:  8478 TCCATTTTGGCGAGTTATCAGTGTTCGGGTCCTCTGCCTTGGCCTGGTAGAGGATCTTCA 8537
```

(b)

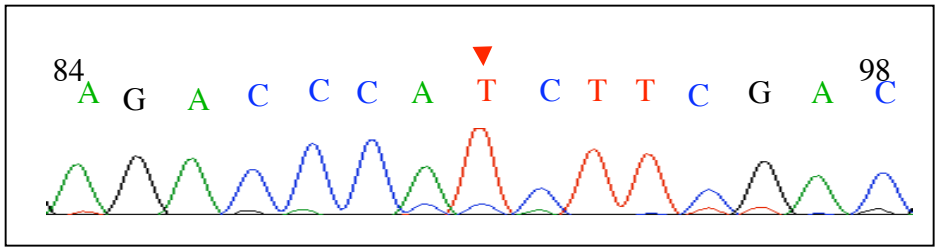

(c)

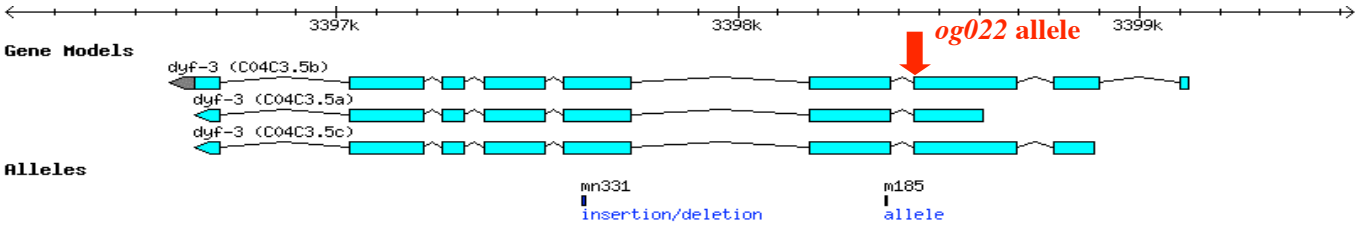

Figure 13. (a) The sequenced region of *dyf-3* (query sequence) containing the *og022* allele, marked with red arrow, along with (b) the chromatogram traces for the region in question. The *og022* allele is located (c) in the first base pair after the third exon of the *dyf-3* gene. Note: *dyf-3* gene runs 3'→5', but the sequence is presented from the positive strand.

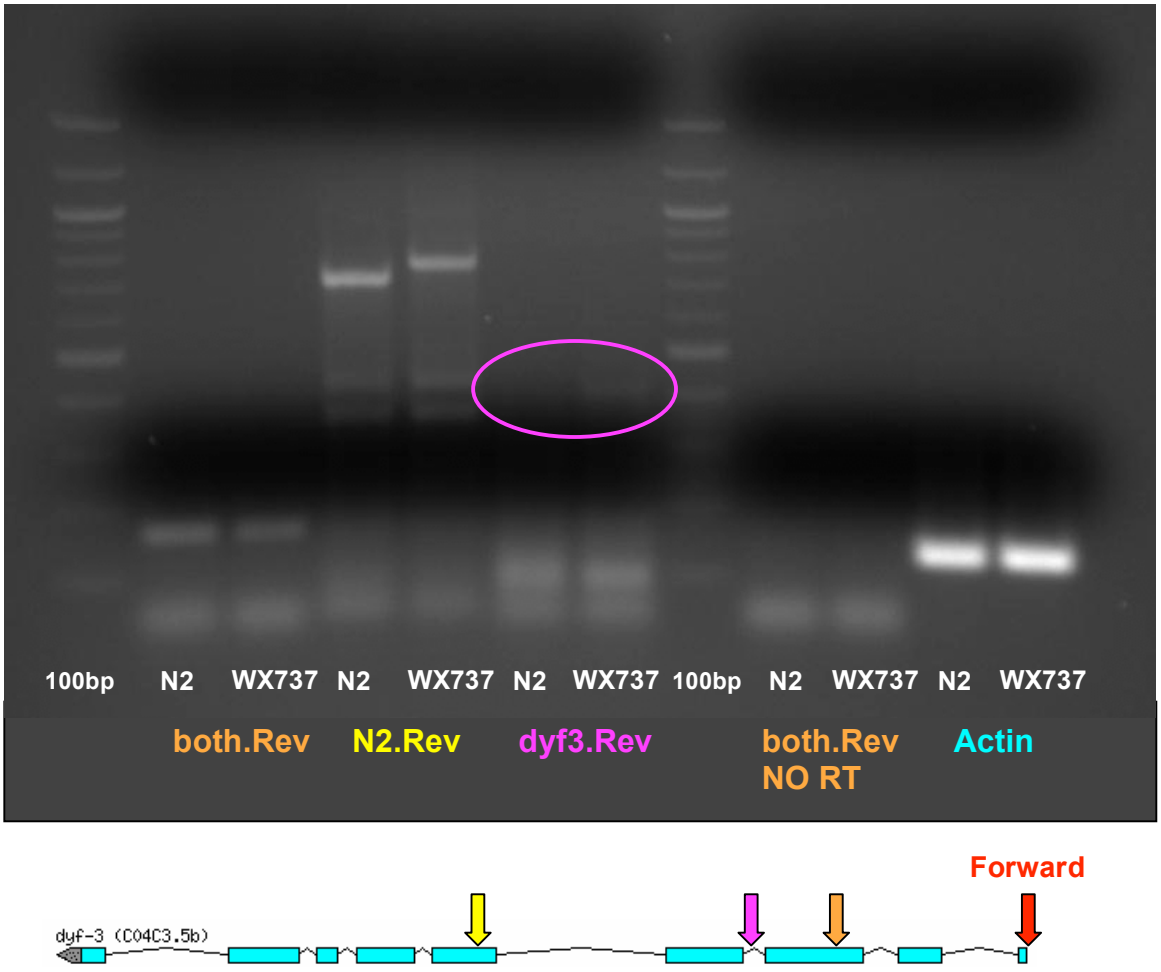

Figure 14. Gel showing RT-PCR reactions of *dyf-3* off N2 and WX737 RNA extractions performed according to Materials and Methods. All reactions used the same Forward primer within the first exon. both.Rev reverse primers were located within the third exon and produce the same length cDNA in N2 and WX737 backgrounds. N2.Rev primers were located within the fifth intron and give a slightly longer cDNA in the WX737 background when compared to N2, due to the third intron being spliced into the mRNA of *dyf-3*. dyf3.Rev primers were located in the third intron which is theoretically spliced into the mRNA of *dyf-3* in the WX737 animal. As indicated, this yields cDNA in the WX737 background, and none in N2. Using both.Rev primers without reverse transcriptase serves as a control for DNA contamination, and actin primers serve as a control for the presence of RNA in the samples.

N2 Product

atgtcgtatcgtgagctgagaaacctgtgtgagatgacgcgaagcctccgataccctcgcttgatgtca
attgagaatttccggaccccaaattttcagctggtggctgaattgctggaatggatcgtgaaaaaatttg
agcccgaatccaaccttgacgcacacgaagtccaaacagaagctgatcgggtcgctttcatcaagaa
cgcggtactcctgatgctccaaaattcgagaatcaagatgaatccaaaaaagttgtaccaggctgatg
gtcatgcggtgcaggaactcctaccggccatgaagatcctctaccaggccaaggcagaggacccg
aacactgataactcgccaaaatggacccaagtcaagaataagctctcgtcgaagatgcaggaggtcc
gaatcactcgtcagctatcatcacaactcccggaaacaggtgccctgctcagtgagctgctgtcccgg
caggagttcatatctcagcaacacgagagagccgcgtcacgggcggtaccacttgctgaggccgag
aaggtgctgcaggcaacagtgcagaacatcgctcaggagactgagcagctatcgaacaagctgaa
caacgtggccagcgatgaggcagagctcgacgagaagatagagcgaaagaagcgagagtacga
gcagttgcaaaaaagattcgcaaagctacagtc

WX737 Product

atgtcgtatcgtgagctgagaaacctgtgtgagatgacgcgaagcctccgataccctcgcttgatgtca
attgagaatttccggaccccaaattttcagctggtggctgaattgctggaatggatcgtgaaaaaatttg
agcccgaatccaaccttgacgcacacgaagtccaaacagaagctgatcgggtcgctttcatcaagaa
cgcggtactcctgatgctccaaaattcgagaatcaagatgaatccaaaaaagttgtaccaggctgatg
gtcatgcggtgcaggaactcctaccggccatgaagatcctctaccaggccaaggcagaggacccg
aacactgataactcgccaaaatggacccaagtcaagaataagctctcgtcgaagatgggtctcacag
gccaccagcctgaaaaagcctgaaaaaactgtcgaaagttcagatgcaggaggtccgaatcactcg
tcagctatcatcacaactcccggaaacaggtgccctgctcagtgagctgctgtcccggcaggagttca
tatctcagcaacacgagagagccgcgtcacgggcggtaccacttgctgaggccgagaaggtgctgc
aggcaacagtgcagaacatcgctcaggagactgagcagctatcgaacaagctgaacaacgtggcc
agcgatgaggcagagctcgacgagaagatagagcgaaagaagcgagagtacgagcagttgcaaa
aaagattcgcaaagctacagtc

Figure 15. Shows the sequencing results of the WX737 and N2 *dyf-3* cDNA bands produced using primers N2.Rev in Figure 14. Exons are indicated by alternating coloration. In the WX737 background, an intron (black) spliced into the mRNA of *dyf-3* after the third intron can be seen. Note: sequences are from the negative strand.

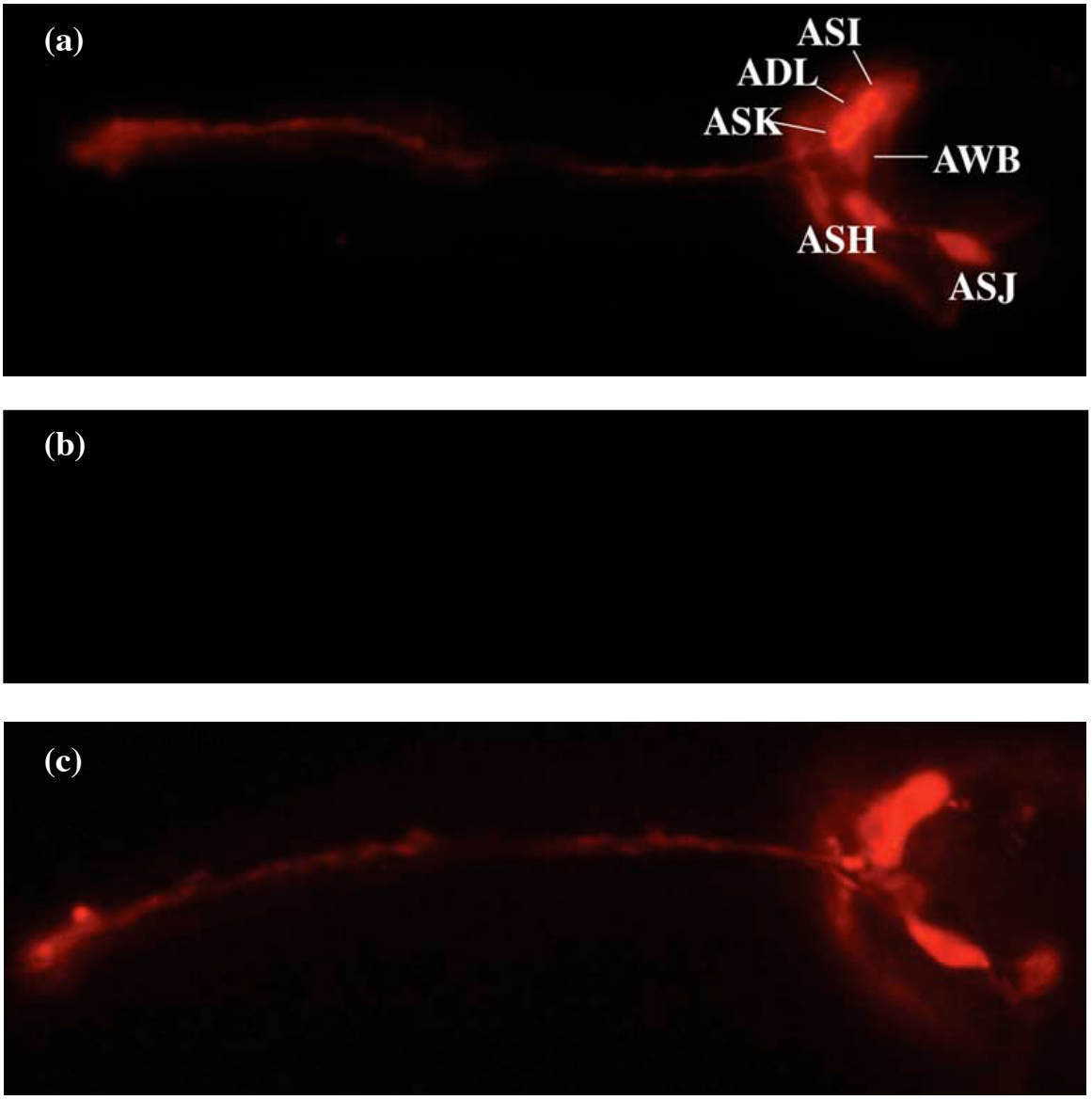

Figure 16. Examples of dye filling patterns in (a) N2 wild-type,
(b) WX737 *dyf-3(og022)*IV, and (c) rescued *dyf-3* mutant backgrounds. The rescue construct and mutant strain in (c) are not those used in this study, but observed phenotypic rescue was similar. As can be seen, microinjecting a wild-type *dyf-3* construct rescues the wild-type dye filling phenotype.

Figure courtesy of:
Murayama, T., Toh, Y., Ohshima, Y., Koga, M. (2005). The dyf-3 gene encodes a novel protein required for sensory cilium formation in Caenorhabditis elegans. *Journal of Molecular Biology*, **346**, 677-687.

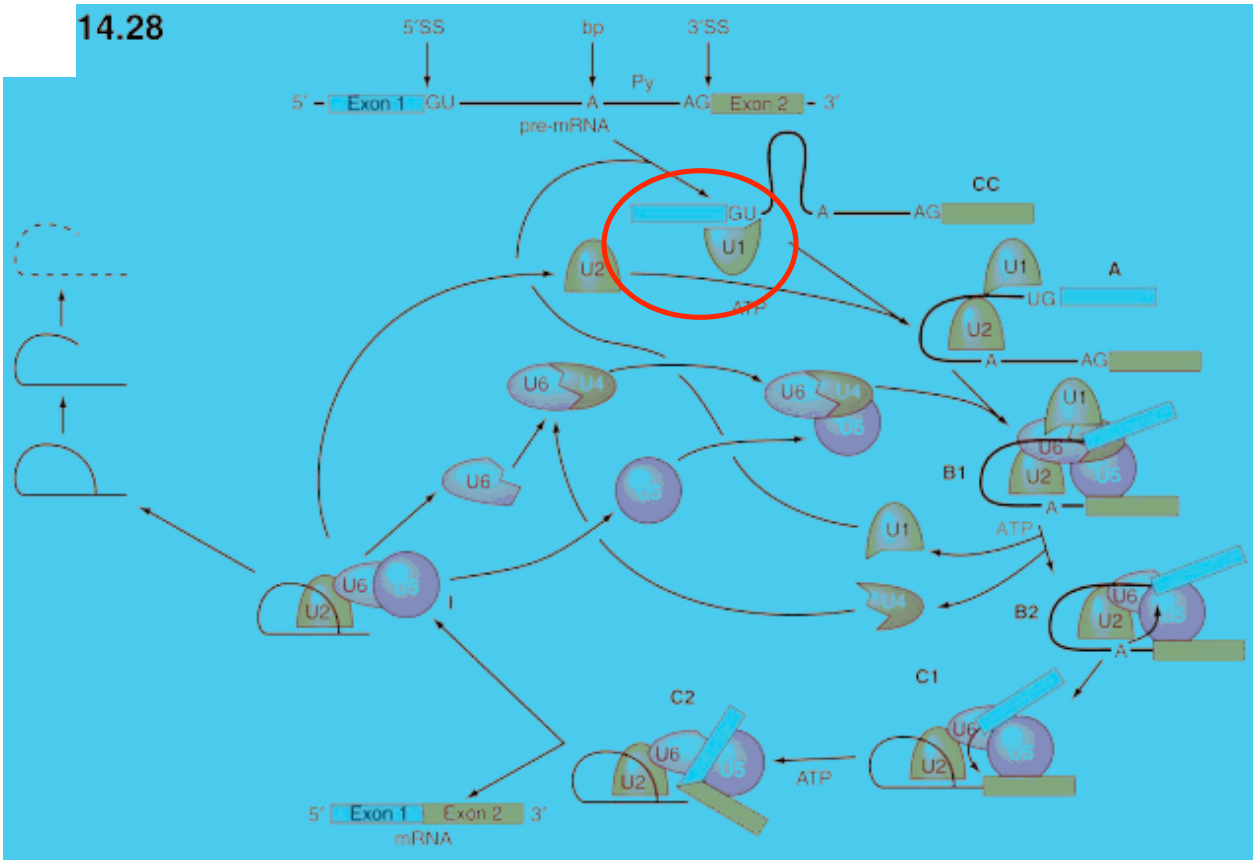

Figure 17. The full eukaryotic spliceosome cycle. Of particular note is the circled recruitment of the U1 snRNP to the 5'ss. It is this interaction which is disrupted by the *og022* allele.

Diagram courtesy of:
Weaver, Robert F. (2005). Molecular Biology, Third Edition, pp. 432-447. McGraw Hill, New York, NY.

References

1. Riddle, D. L., Blumenthal, T., Meyer, B. J., Priess, J. R. (1997). C. elegans II, pp. 1-15. Cold Spring Harbor Laboratory Press, Cold Spring Harbor, NY.

2. Sulston, J. E. and Horvitz, H. R. (1977). Post-embryonic cell lineages of the nematode Caenorhabditis elegans. *Developmental Biology*, **56**, 110-156.

3. The *C. elegans* Sequencing Consortium. (1998). Genome sequence of the nematode C. elegans: A platform for investigating biology. *Science*, **282**, 2012-2018.

4. Riddle, D. L., Blumenthal, T., Meyer, B. J., Priess, J. R. (1997). C. elegans II, pp. 717-726. Cold Spring Harbor Laboratory Press, Cold Spring Harbor, NY.

5. Bray, D. (2001). Cell Movements: From Molecules to Motility, 2nd edit., pp. 225–238, Garland Science, New York, NY.

6. Ibanez-Tallon, I., Heintz, N. & Omran, H. (2003). To beat or not to beat: roles of cilia in development and disease. *Human Molecular Genetics*, **12**, R27–R35.

7. Bargmann, C. I. & Horvitz, H. R. (1991). Chemosensory neurons with overlapping functions direct chemotaxis to multiple chemicals in C. elegans. *Neuron*, **7**, 729–742.

8. Dwyer, N. D., Troemel, E. R., Sengupta, P. & Bargmann, C. I. (1998). Odorant receptor localization to olfactory cilia is mediated by ODR-4, a novel membrane-associated protein. *Cell*, 93, 455–466.

9. Cole, D. G. (1999). Kinesin-II, the heteromeric kinesin. *Cell and Molecular Life Sciences*, **56**, 217-226.

10. Hirokawa, N. (2000). Stirring up development with the heterotrimeric kinesin KIF3. *Traffic*, **1**, 29–34.

11. Marszalek, J. R. & Goldstein, L. S. (2000). Understanding the functions of kinesin-II. *Biochimica et Biophysica Acta*, **1496**, 142–150.

12. Pazour, G. J., Dickert, B. L. &Witman, G. B. (1999). The DHC1b (DHC2) isoform of cytoplasmic dynein is required for flagellar assembly. *Journal of Cell Biology*, **144**, 473–481.

13. Porter, M. E., Bower, R., Knott, J. A., Byrd, P. & Dentler, W. (1999). Cytoplasmic dynein heavy chain 1b is required for flagellar assembly in Chlamydomonas. *Molecular Biology of the Cell*, **10**, 693–712.

14. Cole, D. G., Diener, D. R., Himelblau, A. L., Beech, P. L., Fuster, J. C. & Rosenbaum, J. L. (1998). Chlamydomonas kinesin-II-dependent intraflagellar transport

(IFT): IFT particles contain proteins required for ciliary assembly in Caenorhabditis elegans sensory neurons. *Journal of Cell Biology*, **141**, 993–1008.

15. Cole, D. G. (2003). The intraflagellar transport machinery of Chlamydomonas reinhardtii. *Traffic*, **4**, 435–442.

16. Kozminski, K. G., Johnson, K. A., Forscher, P. & Rosenbaum, J. L. (1993). A motility in the eukaryotic flagellum unrelated to flagellar beating. *Proceedings of the National Academy of Sciences USA*, **90**, 5519–5523.

17. Piperno, G. & Mead, K. (1997). Transport of a novel complex in the cytoplasmic matrix of Chlamydomonas flagella. *Proceedings of the National Academy of Sciences USA*, **94**, 4457–4462.

18. Sloboda, R. D. (2002). A healthy understanding of intraflagellar transport. *Cell Motility and the Cytoskeleton*, **52**, 1–8.

19. Pazour, G. J., Dickert, B. L., Vucica, Y., Seeley, E. S., Rosenbaum, J. L., Witman, G. B. & Cole, D. G. (2000). Chlamydomonas IFT88 and its mouse homologue, polycystic kidney disease gene tg737, are required for assembly of cilia and flagella. *Journal of Cell Biology*, **151**, 709–718.

20. Murcia, N. S., Richards,W. G., Yoder, B. K., Mucenski, M. L., Dunlap, J. R. & Woychik, R. P. (2000). The Oak Ridge polycystic kidney (orpk) disease gene is required for left-right axis determination. *Development*, **127**, 2347–2355.

21. Haycraft, C. J., Swoboda, P., Taulman, P. D., Thomas, J. H. & Yoder, B. K. (2001). The C. elegans homolog of the murine cystic kidney disease gene Tg737 functions in a ciliogenic pathway and is disrupted in osm-5 mutant worms. *Development*, **128**, 1493–1505.

22. Qin, H., Rosenbaum, J. L. & Barr, M. M. (2001). An autosomal recessive polycystic kidney disease gene homolog is involved in intraflagellar transport in C. elegans ciliated sensory neurons. *Current Biology*, **11**, 457–461.

23. Ansley, S. J., Badano, J. L., Blacque, O. E., Hill, J., Hoskins, B. E., Leitch, C. C. et al. (2003). Basal body dysfunction is a likely cause of pleiotropic Bardet-Biedl syndrome. *Nature*, **425**, 628–633.

24. Badano, J. L., Ansley, S. J., Leitch, C. C., Lewis, R. A., Lupski, J. R. & Katsanis, N. (2003). Identification of a novel Bardet-Biedl syndrome protein, BBS7, that shares structural features with BBS1 and BBS2. *American Journal of Human Genetics*, **72**, 650–658.

25. Katsanis, N., Lupski, J. R. & Beales, P. L. (2001). Exploring the molecular basis of Bardet-Biedl syndrome. *Human Molecular Genetics*, **10**, 2293–2299.

26. Mykytyn, K., Nishimura, D. Y., Searby, C. C., Shastri, M., Yen, H. J., Beck, J. S. et al. (2002). Identification of the gene (BBS1) most commonly involved in Bardet-Biedl syndrome, a complex human obesity syndrome. *Nature Genetics*, **31**, 435–438.

27. Nishimura, D. Y., Searby, C. C., Carmi, R., Elbedour, K., Van Maldergem, L., Fulton, A. B. et al. (2001). Positional cloning of a novel gene on chromosome 16q causing Bardet-Biedl syndrome (BBS2). *Human Molecular Genetics*, **10**, 865–874.

28. Blacque, O. E., Reardon, M. J., Li, C., McCarthy, J., Mahjoub, M. R., Ansley, S. J. et al. (2004). Loss of C. elegans BBS-7 and BBS-8 protein function results in cilia defects and compromised intraflagellar transport. *Genes and Development*, **18**, 1630–1642.

29. Li, J. B., Gerdes, J. M., Haycraft, C. J., Fan, Y., Teslovich, T. M., May-Simera, H. et al. (2004). Comparative genomics identifies a flagellar and basal body proteome that includes the BBS5 human disease gene. *Cell*, **117**, 541–552.

30. Perkins, L. A., Hedgecock, E. M., Thomson, J. N. & 686 dyf-3 Acts for Sensory Cilia Formation Culotti, J. G. (1986). Mutant sensory cilia in the nematode Caenorhabditis elegans. *Developmental Biology*, **117**, 456–487.

31. Starich, T. A., Herman, R. K., Kari, C. K., Yeh, W. H., Schackwitz, W. S., Schuyler, M. W. et al. (1995). Mutations affecting the chemosensory neurons of Caenorhabditis elegans. *Genetics*, **139**, 171–188.

32. Brenner, S. (1974). The genetics of Caenorhabditis elegans. *Genetics*, **77**, 71–94.

33. Uchida, O., Nakano, H., Koga, M. & Ohshima, Y. (2003). The C. elegans che-1 gene encodes a zinc finger transcription factor required for specification of the ASE chemosensory neurons. *Development*, **130**, 1215–1224.

34. Wicks, S. R., Yeh, R. T., Gish,W. R.,Waterston, R. H. & Plasterk, R. H. (2001). Rapid gene mapping in Caenorhabditis elegans using a high density polymorphism map. *Nature Genetics*, **28**, 160–164.

35. Sambrook, J. & Russell, D. W. (2001). Molecular Cloning, 3rd edit., Cold Spring Harbor Laboratory Press, Cold Spring Harbor, NY.

36. Mello, C. C., Kramer, J. M., Stinchcomb, D. & Ambros, V. (1991). Efficient gene transfer in C. elegans: extrachromosomal maintenance and integration of transforming sequences. *EMBO Journal*, **10**, 3959–3970.

37. Murayama, T., Toh, Y., Ohshima, Y., Koga, M. (2005). The dyf-3 gene encodes a novel protein required for sensory cilium formation in Caenorhabditis elegans. *Journal of Molecular Biology*, **346**, 677-687.

38. WormBase web site, http://www.wormbase.org, release WS188, date April 16, 2008.

39. Shapiro, M.B., Senapathy, P. (1987). RNA splice junctions of different classes of eukaryotes: Sequence statistics and functional implications in gene expression. *Nucleic Acids Research,* **15**, 7155–7174.

40. Weaver, Robert F. (2005). Molecular Biology, Third Edition, pp. 432-447. McGraw Hill, New York, NY.

41. Haycraft, C. J., Schafer, J. C., Zhang, Q., Taulman, P. D. & Yoder, B. K. (2003). Identification of CHE-13, a novel intraflagellar transport protein required for cilia formation. *Experimental Cell Research*, **284**, 251–263.

42. Swoboda, P., Adler, H. T. & Thomas, J. H. (2000). The RFX-type transcription factor DAF-19 regulates sensory neuron cilium formation in C. elegans. *Molecular Cell*, **5**, 411–421.

43. Collet, J., Spike, C. A., Lundquist, E. A., Shaw, J. E. & Herman, R. K. (1998). Analysis of osm-6, a gene that affects sensory cilium structure and sensory neuron function in Caenorhabditis elegans. *Genetics*, **148**, 187–200.

44. Fujiwara, M., Ishihara, T. & Katsura, I. (1999). A novel WD40 protein, CHE-2, acts cell-autonomously in the formation of C. elegans sensory cilia. *Development*, **126**, 4839–4848.